NEAR-BED TURBULENCE FOR ENTRAINMENT THRESHOLD OF SEDIMENTS

Subhasish Dey, *Chair Professor*

Department of Civil Engineering
Indian Institute of Technology
Kharagpur, West Bengal
INDIA

Present study focuses on

- The time-averaged flow characteristics
- Anisotropy analysis
- Spectral analysis
- Third-order correlations of velocity fluctuations
- Turbulent kinetic energy
- Energy budget
- Bursting parameters

Kline *et al.* (1967) and Robinson, (1991): wall zone is dominated by a sequence of turbulent events, referred to as the bursting phenomenon.

Best (1992): attempted to link the high velocity sweeps with the sediment-entrainment and bed defect.

Krogstad *et al.* (1992) and Papanicolaou *et al.* (2001): presence of bed packing conditions in gravel bed streams affects the turbulence characteristics of the flow and as a result the sediment-entrainment.

Papanicolaou *et al.* (2001): threshold criterion based solely on the time-averaged bed shear stress may under-predict.

Surtherland (1967): sediment threshold is associated with an eddy impact onto the bed to produce a streamwise drag force being large enough enabling to roll the particles about their points of contact.

Heathershaw & Thorne (1985) and Thorne *et al.* (1989): bed-load transport is not correlated with the instantaneous Reynolds shear stress but rather correlated with the near-wall instantaneous streamwise velocity.

Drake *et al.* (1988): majority of the sediment transport is associated with sweep events. These events occur for a small fraction of time at any particular location of the bed.

Song *et al*. (1994): time-averaged turbulence characteristics over a mobile gravel bed have slight difference from their traditional values over a rigid rough bed.

Cao (1997): proposed a model for the sediment-entrainment based on the main characteristics of the bursting structures (with time and spatial scaling) inherent in wall turbulent flows.

Papanicolaou (2000): entrainment threshold correlates well with the streamwise velocity.

Nikora & Goring (2000): characteristics of turbulence in flows over weakly mobile beds is different from those over immobile beds and beds with intense bed-load transport.

Sumer *et al.* (2003): sediment transport increases markedly with an increase in turbulent level.

Dey & Raikar (2007): presented time-averaged velocity, turbulence intensities and the Reynolds shear stresses in flows over gravel beds at the near-threshold of motion.

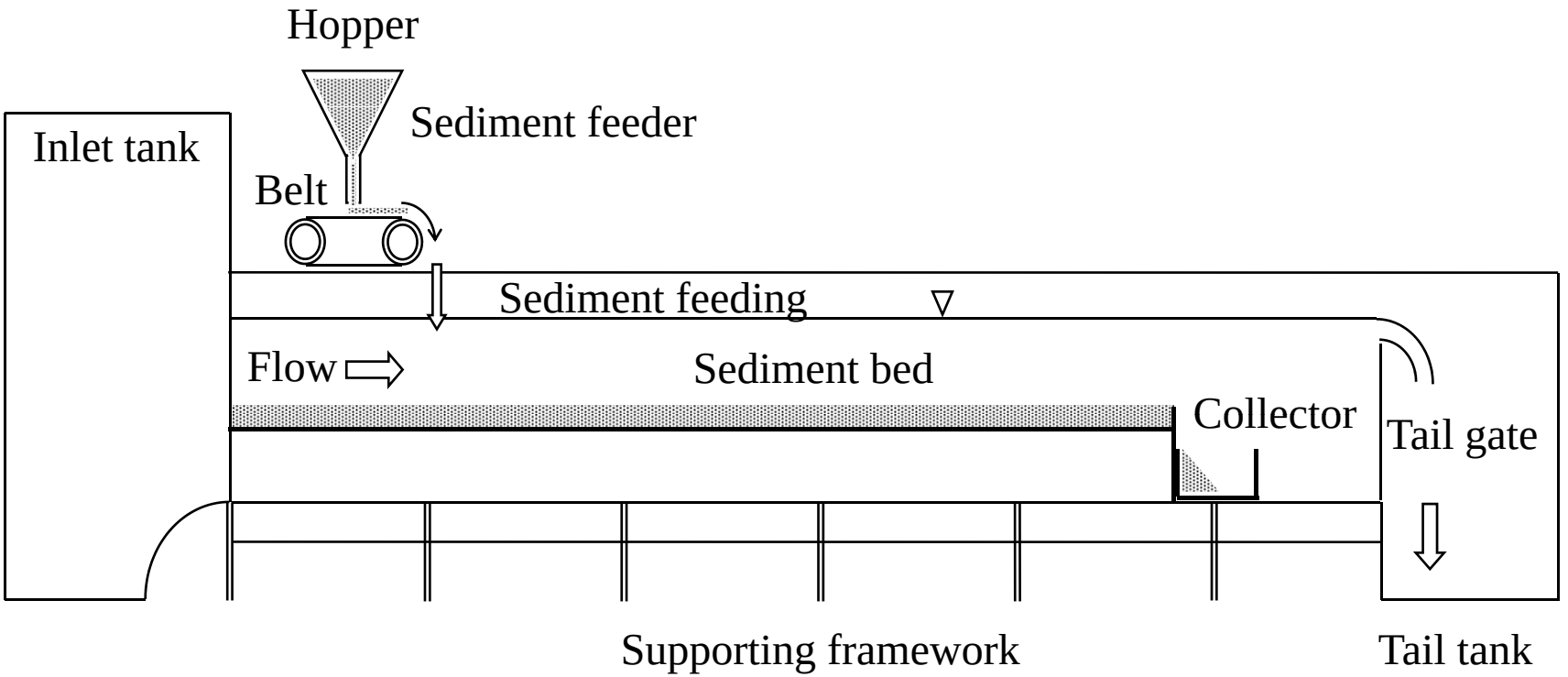

Schematic of experimental setup

d_{50} (mm)	Relative density	σ_g	Angle of repose (deg)	u_{*c} (m/s)
1.97	2.65	1.28	29	0.036
2.92	2.65	1.2	30	0.046
4.1	2.65	1.13	32.5	0.058
5.53	2.65	1.1	34	0.07

In the above, u_{*c} is the critical shear velocity obtained from the Shields diagram

Table 1. Characteristics of sediments used in the experiments

Set	Bed condition	d_{50} (mm)	S (%)	h (m)	U (m/s)
1	Immobile	1.97	0.083	0.14	0.49
	Entrainment	1.97	0.083	0.215	0.61
2	Immobile	2.92	0.143	0.12	0.54
	Entrainment	2.92	0.143	0.15	0.63
3	Immobile	4.1	0.143	0.13	0.6
	Entrainment	4.1	0.143	0.23	0.77
4	Immobile	5.53	0.286	0.12	0.66
	Entrainment	5.53	0.286	0.185	0.81

Table 2. Experimental parameters

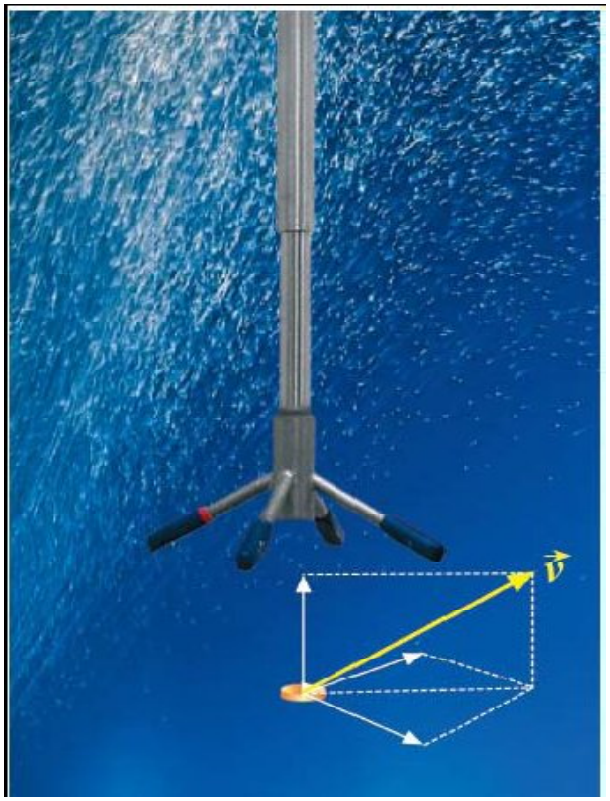

- A high-resolution acoustic velocimeter

- Used to measure 3D water velocity in a wide variety of applications from the laboratory to the field with an acoustic frequency of 10 MHz.

5-cm Down looking Vectrino (3D water velocity sensor)

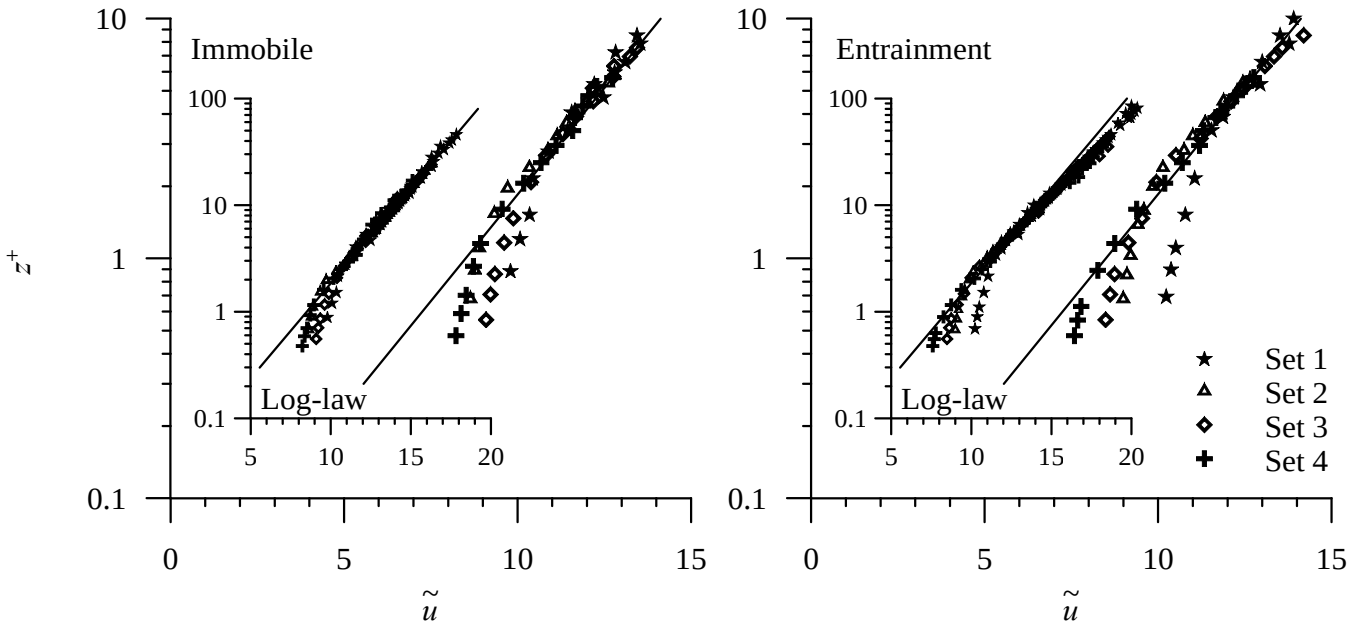

Vertical distributions of $\tilde{u}$

- In near-bed flow zone, there exists a departure in the distributions of the time-averaged streamwise velocity from the logarithmic law due to the roughness layer created by the sediment particles.

- Departure of data plots for immobile beds from the logarithmic law is higher than that for entrainment threshold beds.

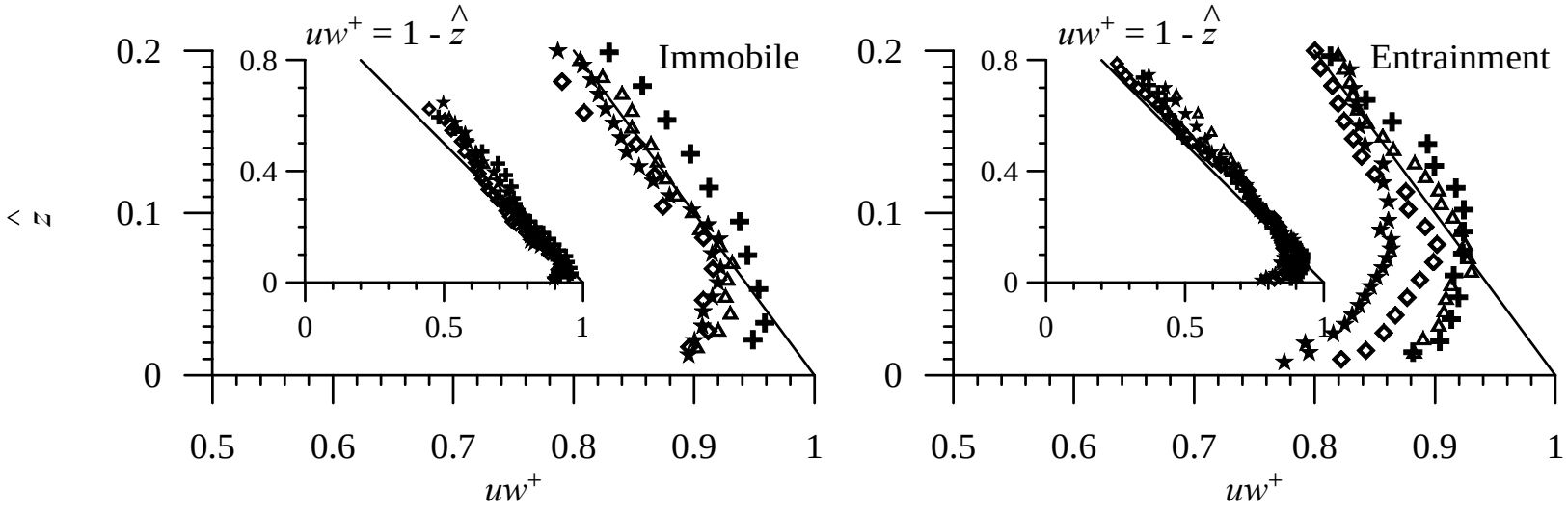

Vertical distributions of uw^+

- Near the bed, normalised Reynolds shear stress for immobile and entrainment threshold beds have a strong departure from the linear law.
- Away from the bed, they are reasonably consistent with the linear law, although there is a slight tendency to overestimate the law.
- Near the bed, distributions of normalised Reynolds shear stress for entrainment threshold beds diminishes more than that for immobile beds.

- The reduction of u_* for entrainment threshold beds is due to a portion of the fluid turbulent stress transferred to the bed particles to overcome the frictional resistance at the contacts of the entrained sediment particles

- The damping of the Reynolds shear stress is associated with the provided momentum for the flow to maintain their motion.

- The total bed shear stress is balanced by the sum of the bed shear stress in fluid τ_f and that in particles τ_s to overcome frictional resistance. Therefore, $\tau_s = \tau - \tau_f$

$$\tau_s = \mu(1-s)\rho g\,(\pi d_{50}^3/6)\xi n \text{ and } \tau - \tau_f = \rho\,(u_{*1}^2 - u_{*2}^2)$$

μ = Coulomb friction factor = $\tan\phi$

ϕ = angle of internal friction

s = relative density of sediments

ξ = fraction of particles entrained per unit area

n = number of bed particles per unit area, that is $(1-\rho_0)/(\pi d_{50}^2/4)$

ρ_0 = porosity of sediments.

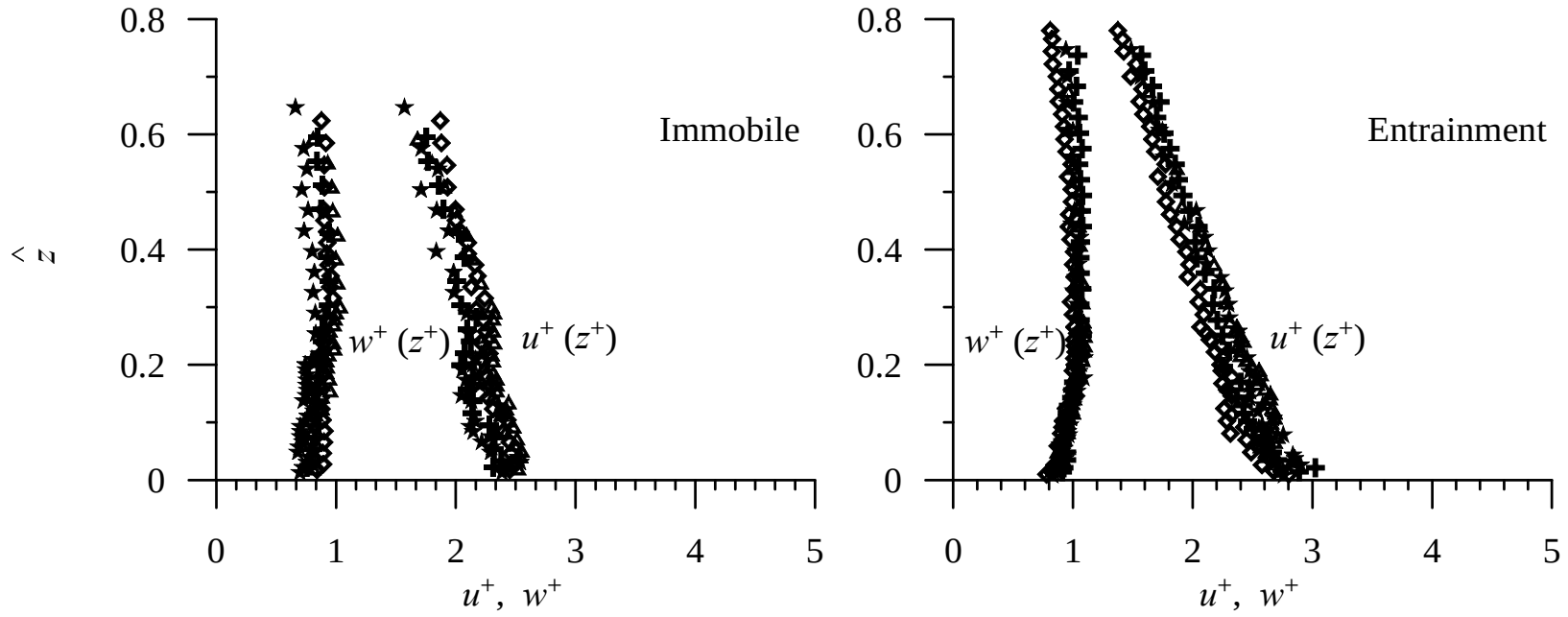

Vertical distributions of normalised u^+ and w^+

- In general, the distributions of streamwise turbulent intensity for entrainment threshold beds exceed those for immobile beds within the wall-shear layer ($z/h < 0$).

- Outside the wall-shear layer, w^+ becomes almost unity in conformity with Grass (1971).

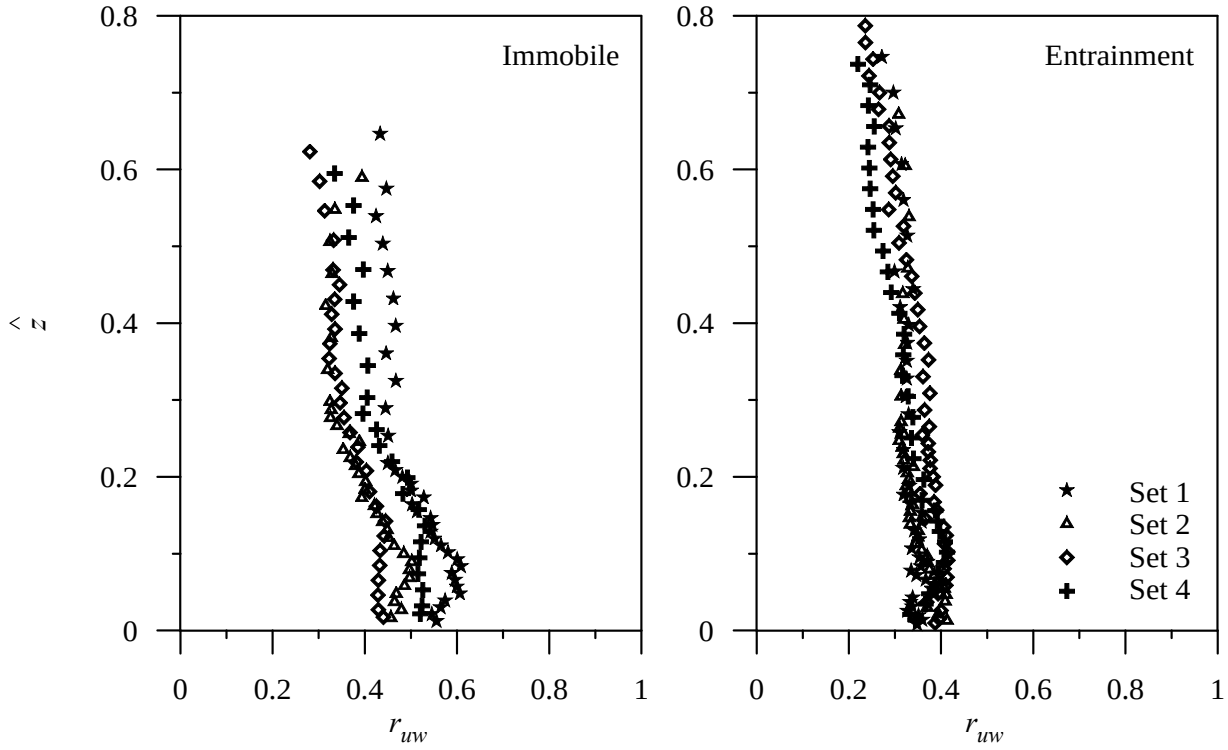

Vertical distributions of correlation coefficient, r_{uw}

- The depth-averaged value of r_{uw} is 0.45 for immobile beds and 0.4 for entrainment threshold beds.

- Hinze (1975) and Schlichting (1979) obtained $r_{uw} = 0.4 – 0.5$ over most of the extent of the boundary layer flows over smooth beds.

- For weekly mobile rough beds, Dey & Raikar (2007) reported that a nearly constant value of $r_{uw} \approx 0.43$ exists for $z/h < 0.6$, but it decreases for $z/h > 0.6$.

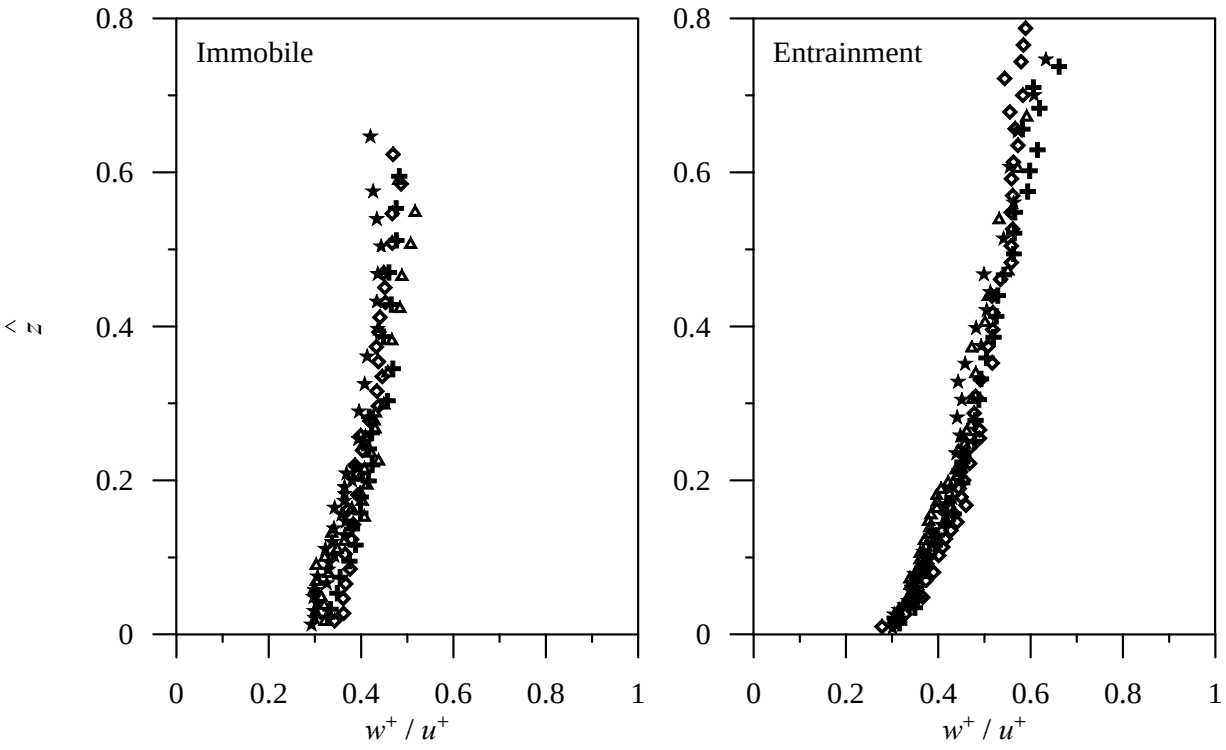

Vertical distributions of ratio of vertical to streamwise turbulence intensity w^+/u^+

- The ratio w^+/u^+ is about 0.3 near the bed, varying almost linearly with z/h and reaching to 0.5 at $z/h = 0.6$.

- The ratio w^+/u^+ in flows over immobile and entrainment threshold beds remains less than those observed by Nezu & Nakagawa (0.55 for smooth bed) and Dey & Raikar (0.6 for weakly mobile bed).

Anisotropy Analysis

Reynolds stress anisotropy tensor b_{ik} is defined as the difference between the ratio of Reynolds tensor terms to the turbulent kinetic energy and its isotropic equivalent quantity (Lumley & Newman, 1977; Lumley, 1978).

$$b_{ik} = \overline{u_i' u_k'} / (2q) - \delta_{ik} / 3$$

where q is the average turbulent kinetic energy δ_{ik} is the Kronecker delta function $\delta_{ik} = 0$ if $i \neq k$, or 1 if $i = k$.

Limits of 1D and 2D turbulence are given by the upper linear boundary that is

$$II = \left(b_{ik} b_{ik} / 2 \right), \quad III = b_{ij} b_{jk} b_{ki} / 3$$ while the first invariant is zero ($I = b_{ii} = 0$).

A cross-plot of $-II$ against III is termed as *anisotropic invariant map* (AIM).

In an AIM, $-II$ (positive or zero) represents the degree of anisotropy and III refers to the nature of anisotropy.

for one-dimensional turbulence: $II = (8/3),\quad III = (16/9)$

for two-dimensional turbulence: $II = (2/3),\quad III = (-2/9)$

for three-dimensional turbulence: $-II = III = 0$

Another method to estimate the overall anisotropy in the Reynolds stress tensor is given by the invariant function as: F (= $1 + 9II + 27III$)

F = 0 for two-dimensional isotropic state and F = 1 three-dimensional isotropic state.

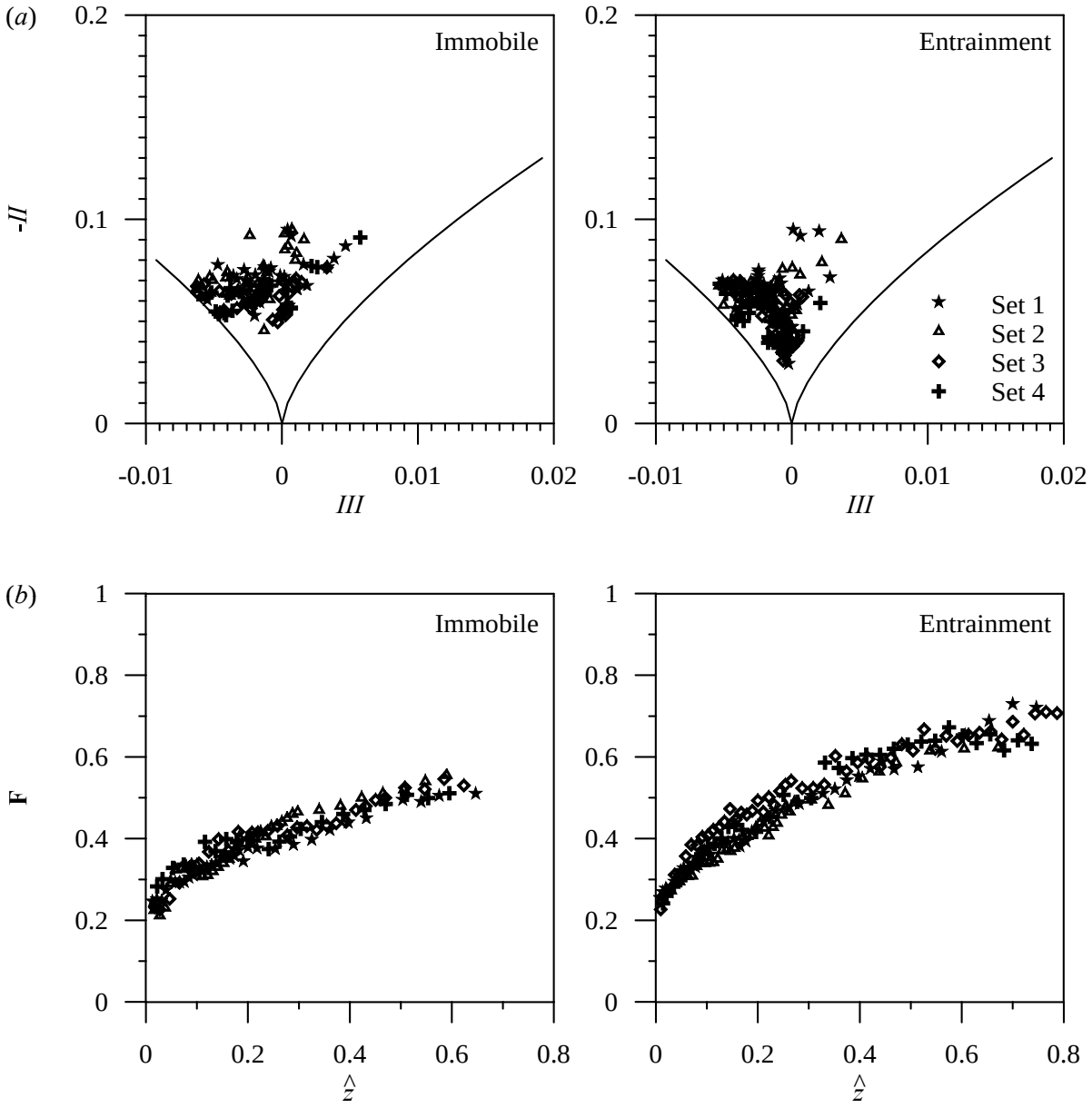

(a) Anisotropy invariant maps (AIM)

(b) Vertical distributions of anisotropy invariant function, F

- The data plots collapse on a band across the flow layers, where the values of F approach closer to unity in the flows over entrainment threshold beds than those over immobile beds.

- It suggests that the turbulence in flows over entrainment threshold beds satisfy isotropy better that over immobile beds.

Spectral analysis

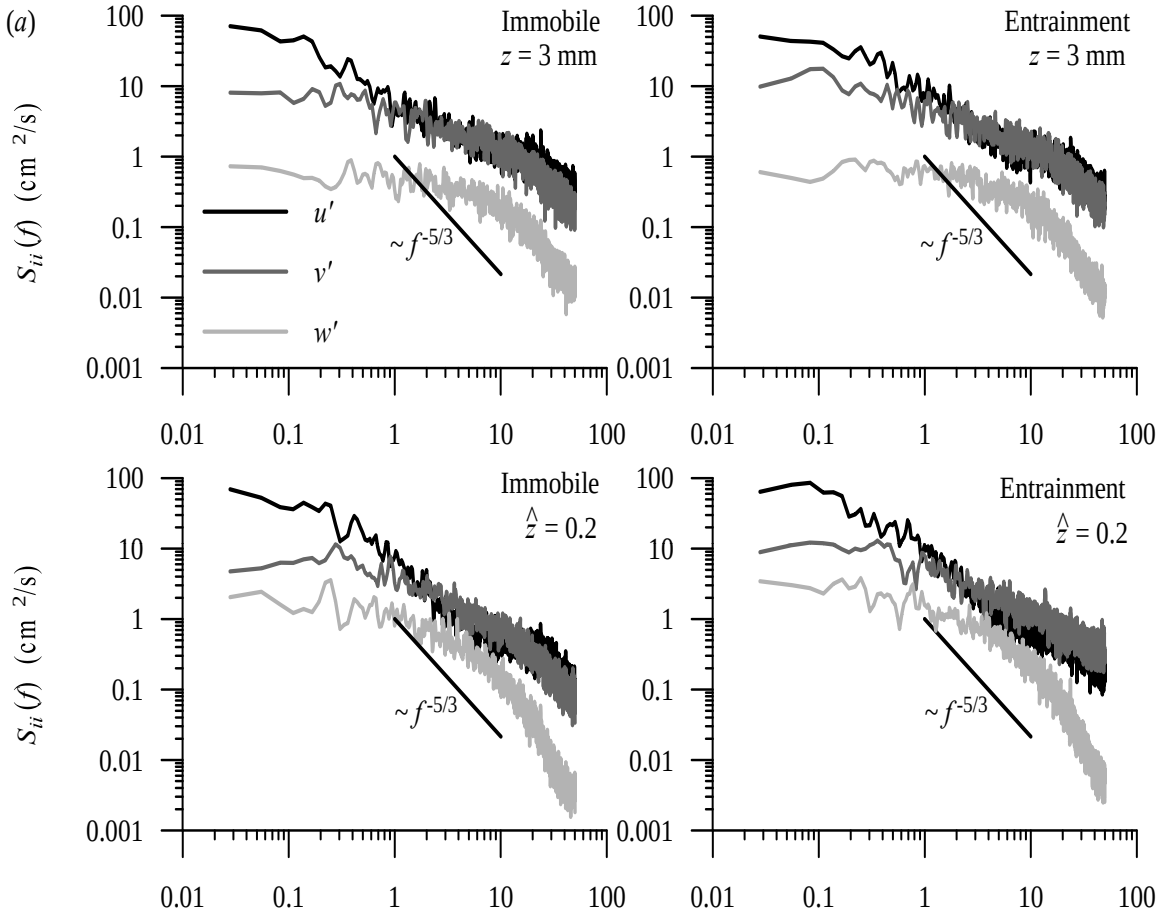

Velocity power spectra $S_{ii}(f)$

Set 1 data are used

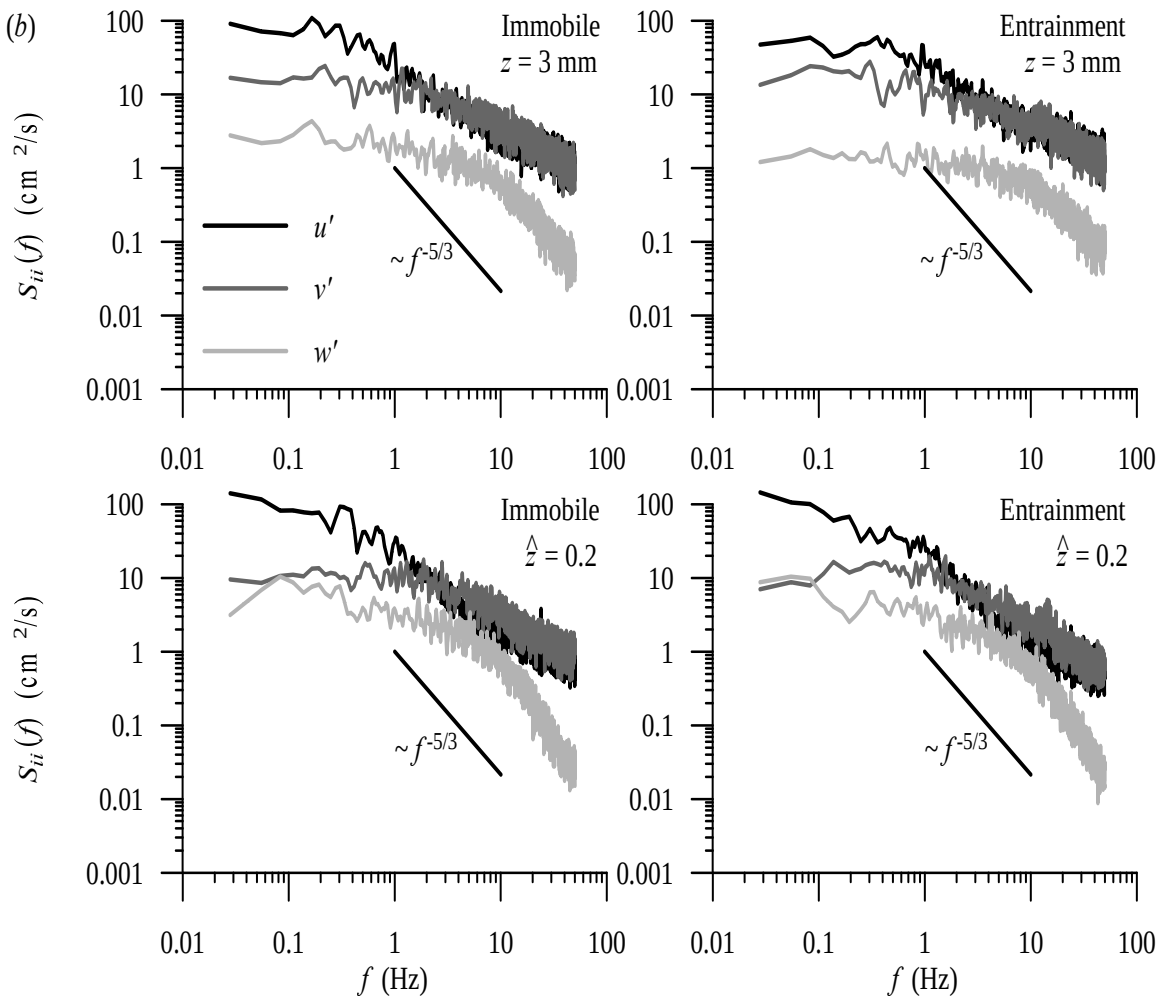

Velocity power spectra $S_{ii}(f)$

Set 4 data are used

Spectral analysis

- Using discrete fast Fourier transforms of each data series, velocity power spectra $S_{ii}(f)$ were calculated.

- All velocity spectra display portions of constant $f^{-5/3}$ slope at higher frequencies suggestive of the inertial subrange.

- At low frequencies, velocity spectral power exhibits similar relationships between velocity components, in which $S_{uu}(f) > S_{vv}(f) > S_{ww}(f)$.

- The velocity power spectra is not influenced by the movement of the sediment particles.

Third-order Correlations of Velocity Fluctuations :

Third-order correlations are directly correlated to the turbulent coherent structures due to preservation of their signs.

The set of third-order correlations M_{jk} are expressed as:

$$M_{jk} = \overline{\tilde{u}^j \tilde{w}^k}$$

$$M_{30} = \overline{\tilde{u}^3} = \overline{u'u'u'} / \left(\overline{u'u'}\right)^{1.5} \qquad M_{03} = \overline{w'w'w'} / \left(\overline{w'w'}\right)^{1.5}$$

$$M_{21} = \overline{u'u'w'} / \left(\overline{u'u'}\right) \times \left(\overline{w'w'}\right)^{0.5} \qquad M_{12} = \overline{u'w'w'} / \left(\overline{u'u'}\right)^{0.5} \times \left(\overline{w'w'}\right)$$

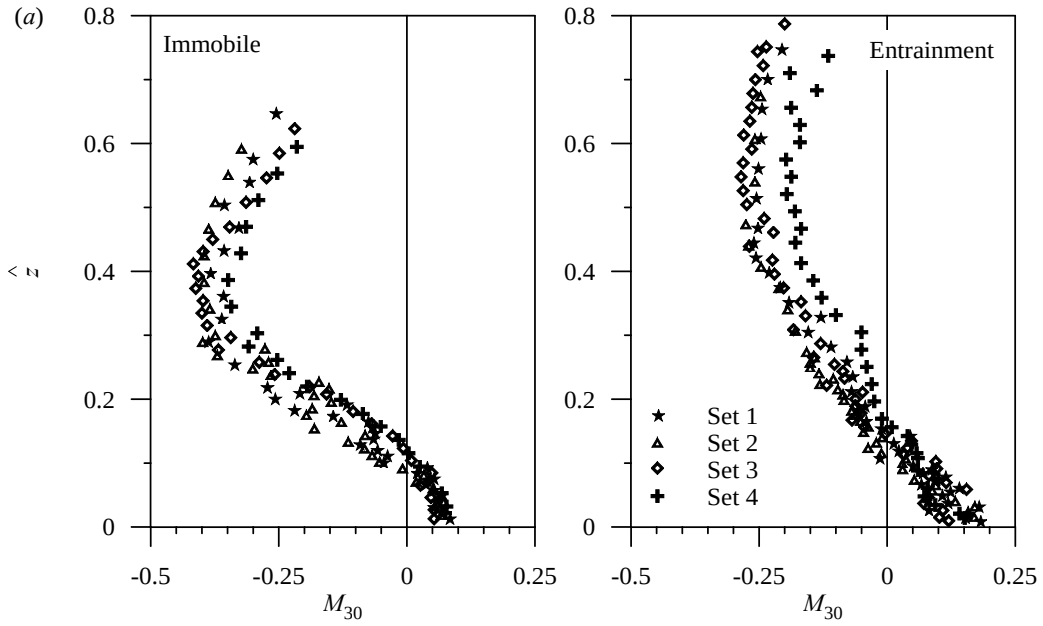

(A) M_{30}

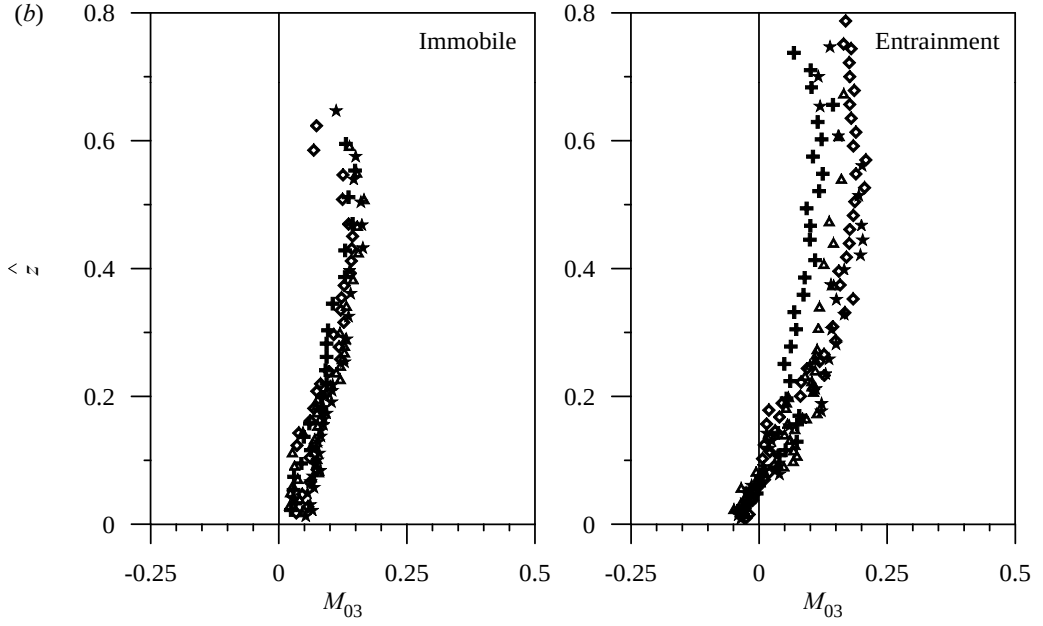

(B) M_{03}

Distributions of third-order correlations, skewness

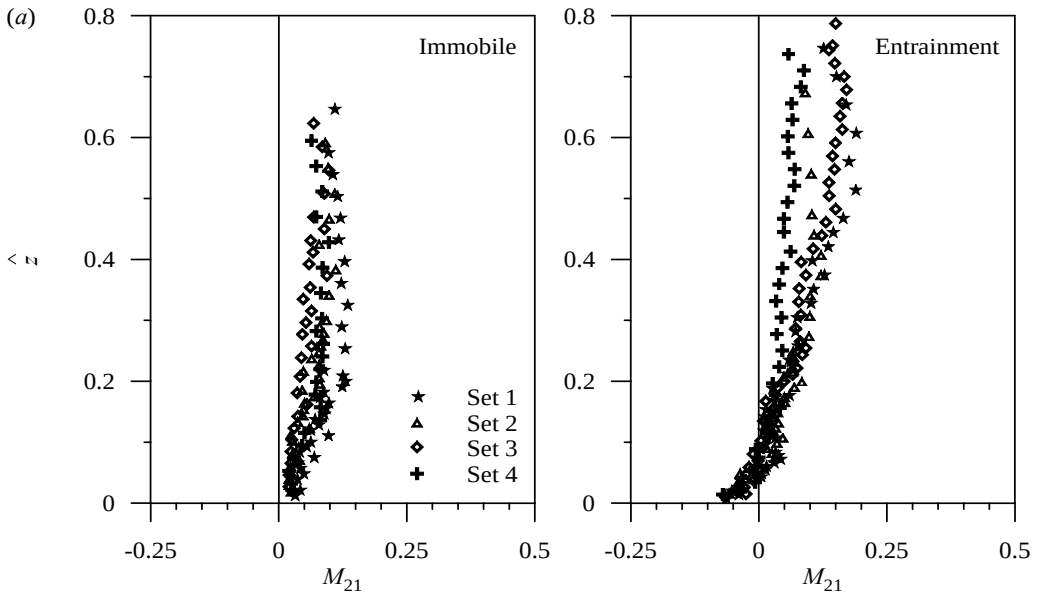

(A) M_{21}

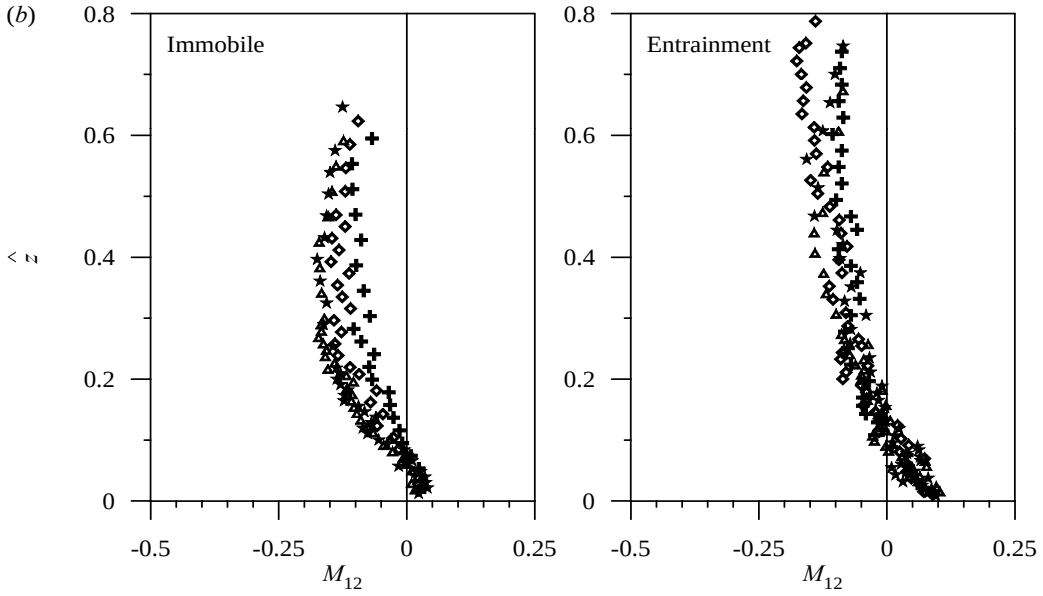

(B) M_{12}

Distributions of third-order correlations (advection of Reynolds normal stresses)

- The mean trends of M_{03} and M_{21} are positive for the entire depth in flows over immobile beds, whilst those are negative near the bed ($z/h < 0.08$) and positive for $z/h > 0.08$ in flows over entrainment threshold beds. It means the flux of $\overline{u'u'}$ and the advection of $\overline{w'w'}$ are in downward direction in the near-bed flow zone over entrainment threshold beds.

- Across the entire flow depth for immobile beds, the flux of $\overline{w'w'}$ and the advection of $\overline{u'u'}$ are in upward direction and the same is attributed to the flow zones for $z/h > 0.08$ for entrainment threshold beds.

Turbulent Kinetic Energy :

The vertical distributions of streamwise and vertical flux of the nondimensional turbulent kinetic energy are defined as:

F_{ku} ($=f_{ku}/u_*^3$) and F_{kw} ($=f_{kw}/u_*^3$)

The streamwise and vertical flux of the turbulent kinetic energy are expressed as:

$$f_{ku} = 0.75\left(\overline{u'u'u'} + \overline{u'w'w'}\right)$$

and $$f_{kw} = 0.75\left(\overline{w'w'w'} + \overline{w'u'u'}\right)$$

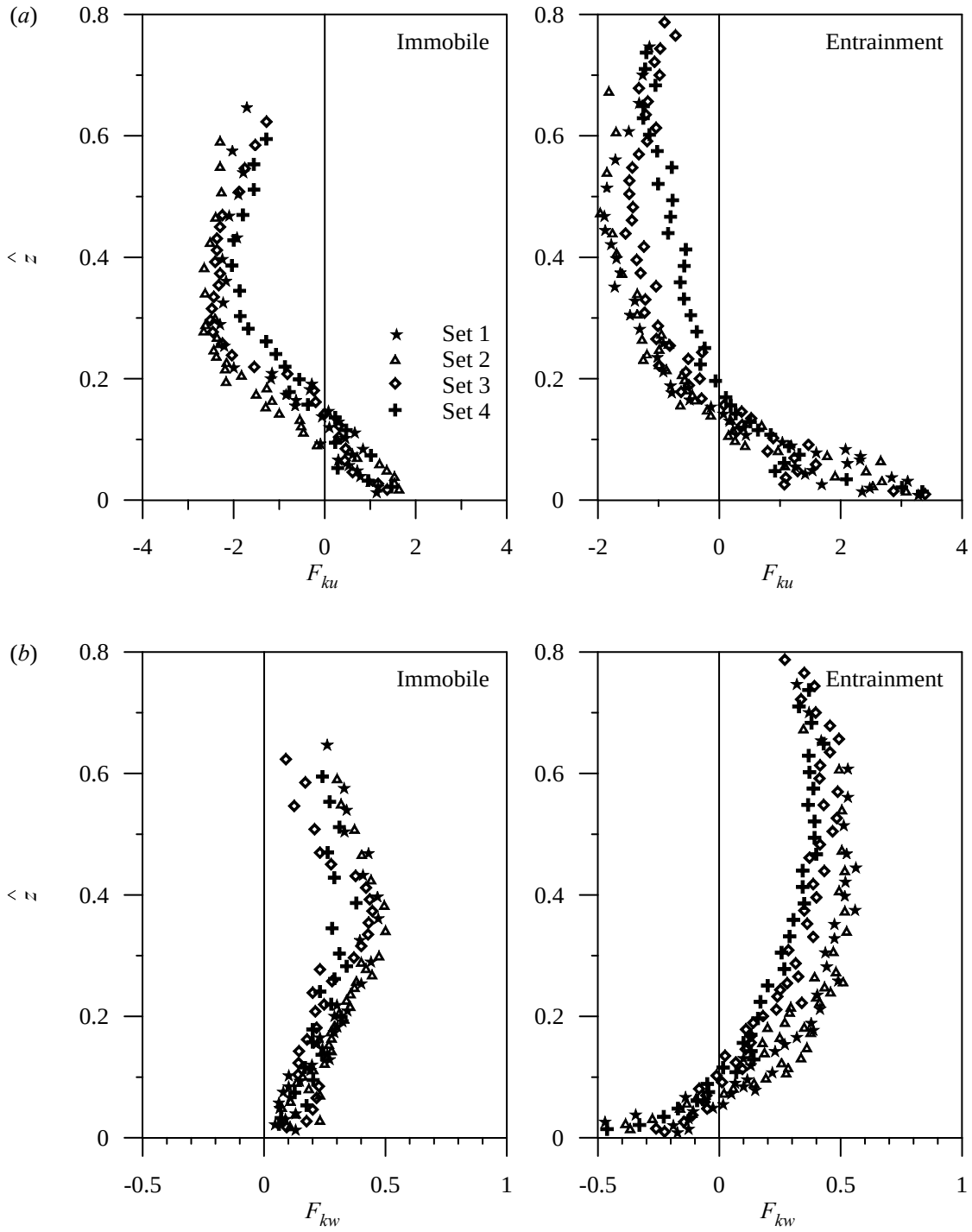

(A) Distributions of streamwise flux of turbulent kinetic energy F_{ku}

(B) Distributions of vertical flux of turbulent kinetic energy F_{kw}

The increased near-bed positive value of streamwise flux of turbulent kinetic energy and the negative value of vertical flux of turbulent kinetic energy are associated with the sediment-entrainment.

Energy Budget

Turbulent production : $t_P = -\overline{u'w'}\left(\partial u / \partial z\right)$

Turbulent energy diffusion : $t_D = \partial f_{kw} / \partial z$

Viscous diffusion : $v_D = \text{-}\upsilon\left(\partial^2 k / \partial z^2\right)$

Turbulent dissipation : $\varepsilon = \left(15\upsilon / u^2\right)\overline{(\partial u' / \partial t)^2}$

Pressure energy diffusion : $P_D = \partial\left(\overline{p'w'} / \rho\right) / \partial z$

The turbulent energy budget relationship : $p_D = t_P - \varepsilon - t_D$

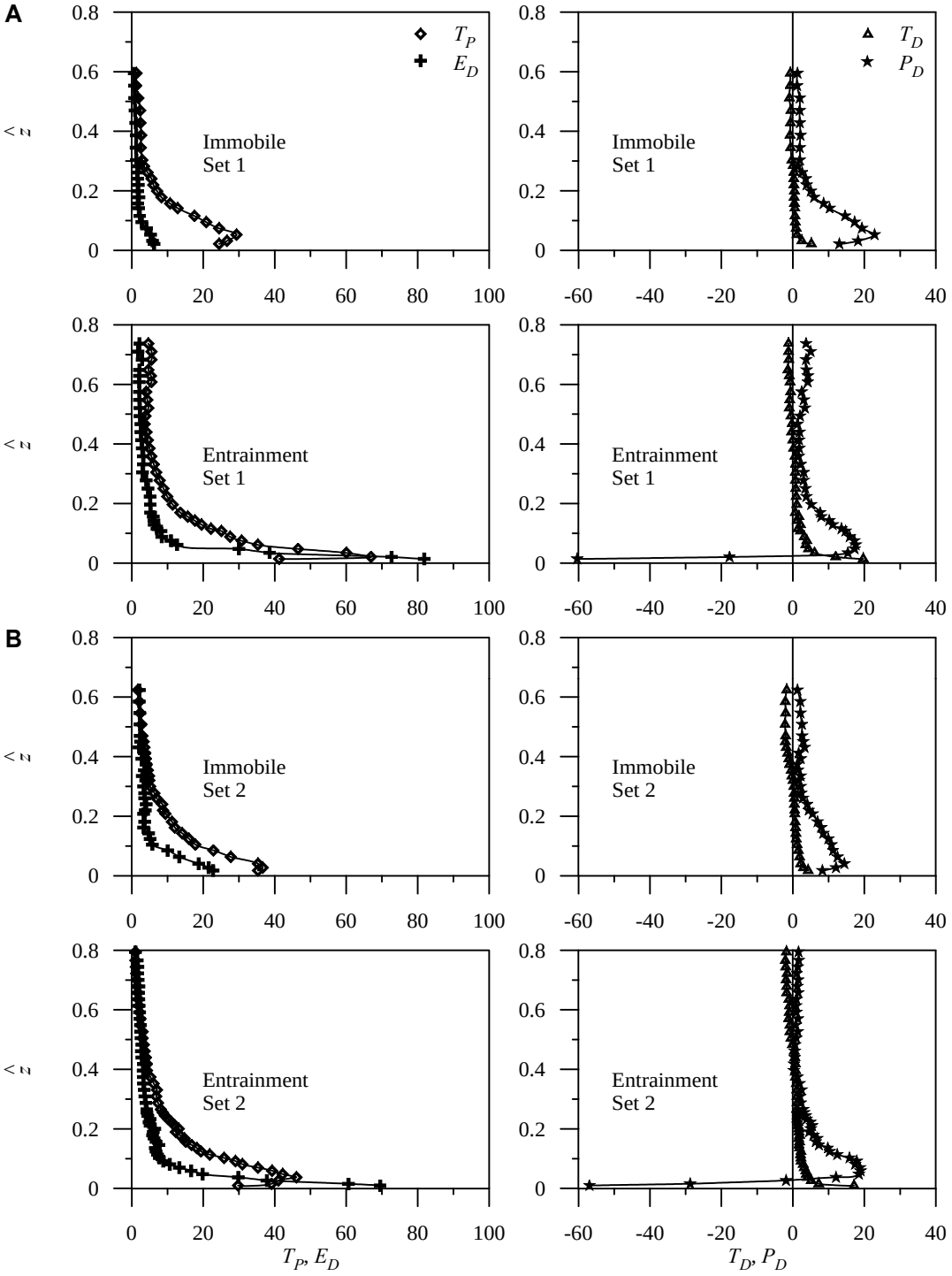

Turbulent energy budget (A) Set 1.

Turbulent energy budget (B) Set 2.

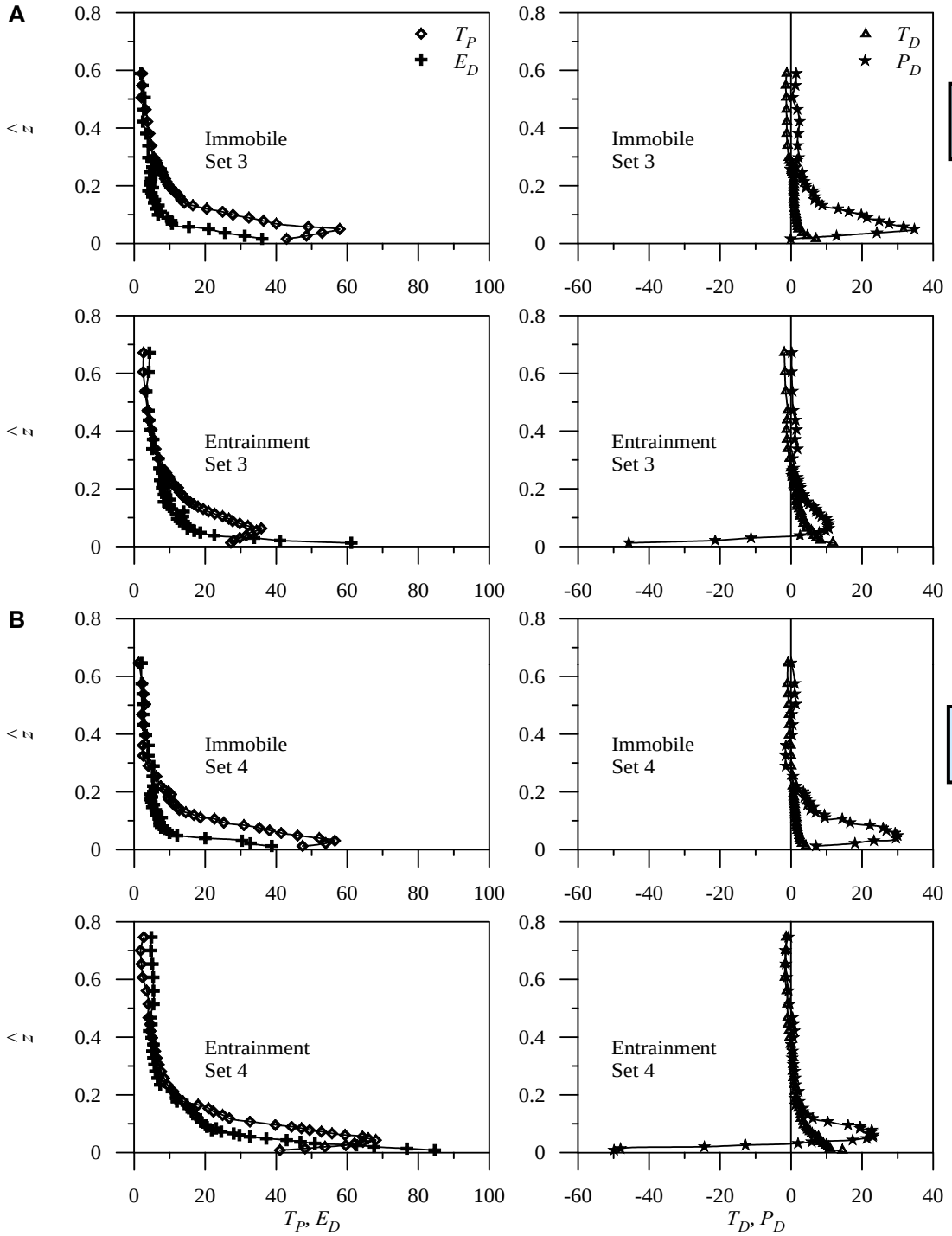

Turbulent energy budget (A) Set 3

Turbulent energy budget (A) Set 4

In the near-bed flows over entrainment threshold beds, the turbulent dissipation exceeds the turbulent production and the pressure energy diffusion is considerably negative.

Quadrant Analysis:

A simple method for the quantitative assessment of the coherent structures is the quadrant analysis.

Four quadrants are defined as:

- $Q1$, first-quadrant $(u'\,w')_1$, where $u'>0$ and $w'>0$, denoting an event in which high speed fluid moves toward the centre of the flow field (outward interaction).

- $Q2$, second-quadrant $(u'\,w')_2$, where $u'<0$ and $w'>0$, denoting an event in which low-speed fluid moves toward the centre of the flow field, away from the wall (ejection).

- $Q3$, third-quadrant $(u'\,w')_3$, where $u'<0$ and $w'<0$, denoting an event in which low-speed fluid moves toward the wall (inward interaction); and

- $Q4$, fourth-quadrant $(u'\,w')_4$, where $u'>0$ and $w'<0$, denoting an event in which high-speed fluid moves toward the wall (sweep).

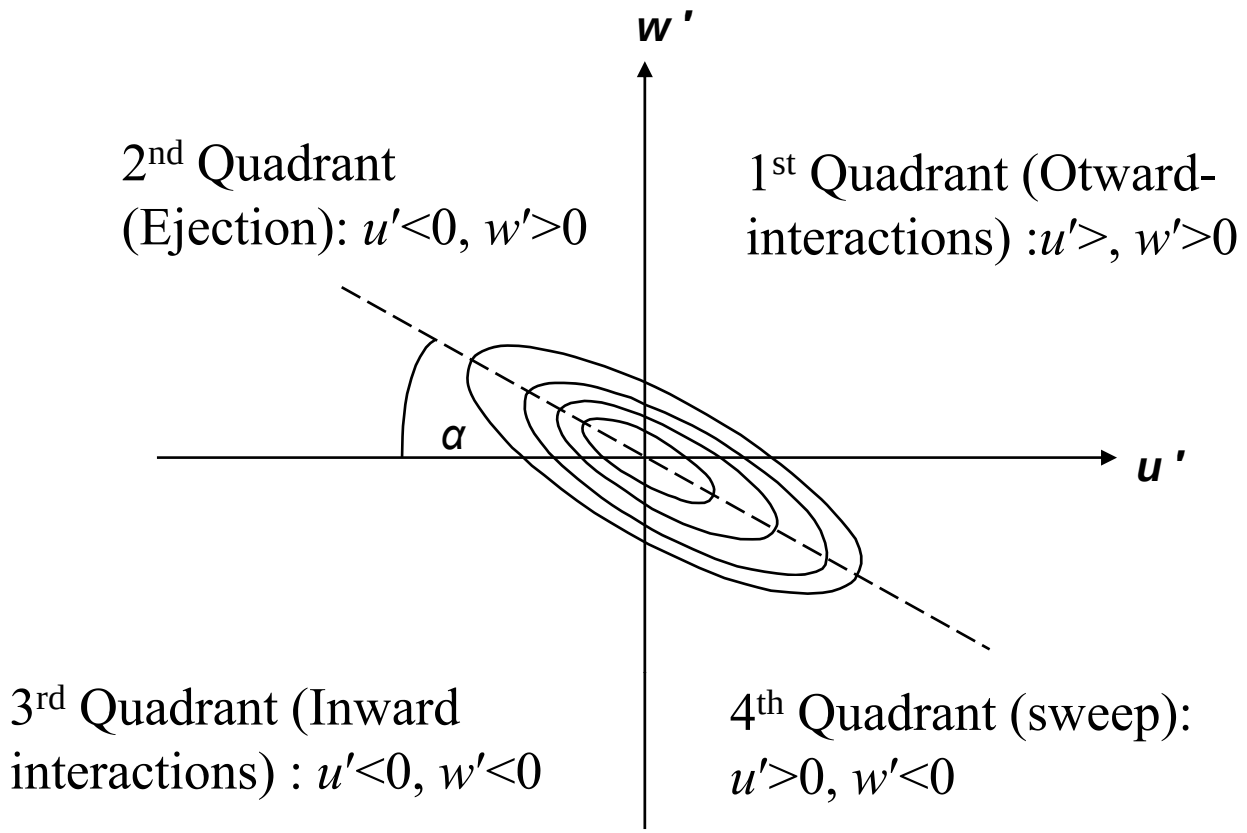

Joint probability function of the location of the velocity fluctuation vector in the (u', w') plane

A detection function is given by:

$$\lambda_{i,H}(z,t) = \begin{cases} 1, & \text{if } (u',w') \text{ is in quadrant } i \text{ and if } \left|u'w'\right| \geq H(\overline{u'u'})^{0.5}(\overline{w'w'})^{0.5} \\ 0, & \text{otherwise} \end{cases}$$

the contributions to $-\overline{u'w'}$ from the quadrant i outside the hole region of size H is estimated by

$$\left\langle u'w' \right\rangle_{i,H} = \lim_{T\to\infty} \frac{1}{T} \int_0^T u'(t)w'(t)\lambda_{i,H}(z,t)dt$$

Thus, the fractional contribution $S_{i,H}$ to $-\overline{u'w'}$ form each event is:

$$S_{i,H} = \frac{\left\langle u'w' \right\rangle_{i,H}}{\overline{u'w'}}$$

The sum of contributions from different bursting events at a point is unity, that is

$$\sum_{i=0}^{i=4} [S_{i,H}]_{H=0} = 1$$

Net effect of Q_2 and Q_4 events, $\Delta S_{i,H} = S_{4,H} - S_{2,H}$

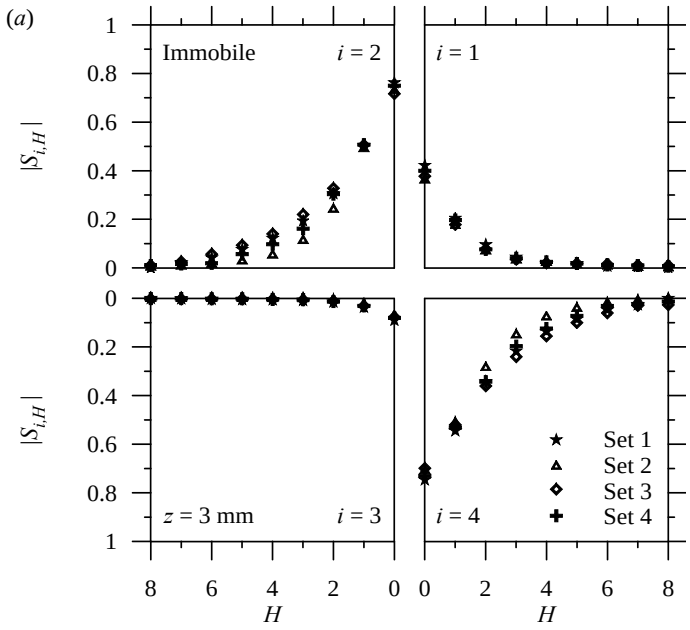

(A) Immobile bed

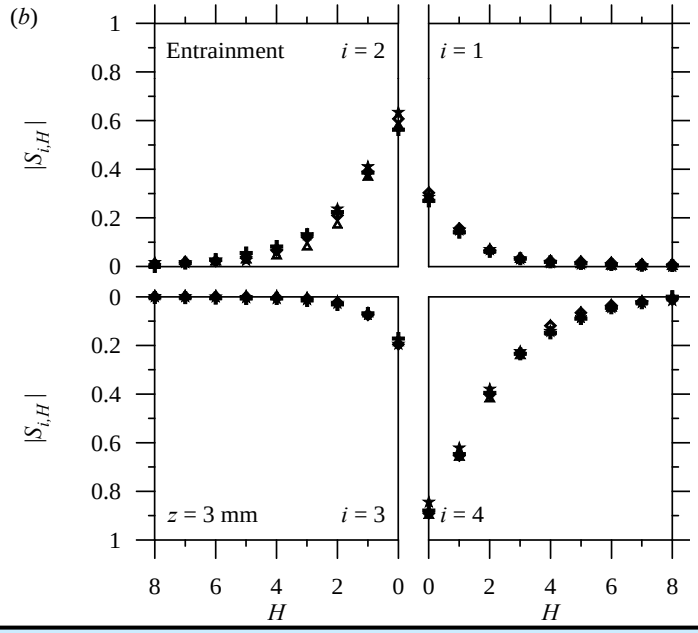

(B) Entrainment threshold bed

Variations of $|S_{i,H}|$ with H at $z = 3$ mm

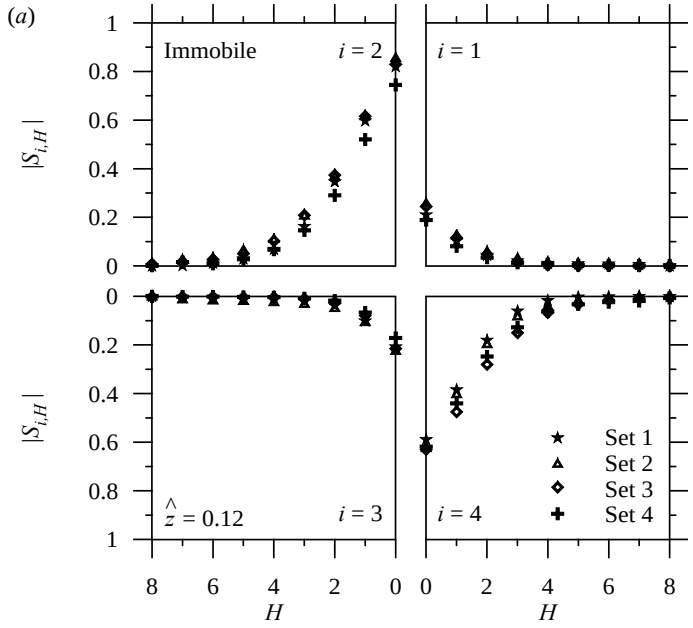

(A) Immobile bed

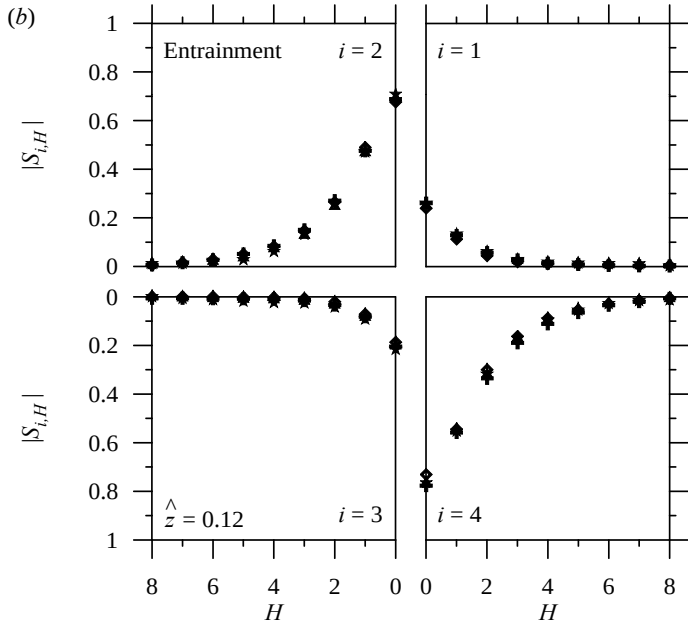

(B) Entrainment threshold bed

Variations of $|S_{i,H}|$ *w*ith H at $z/h = 0.12$

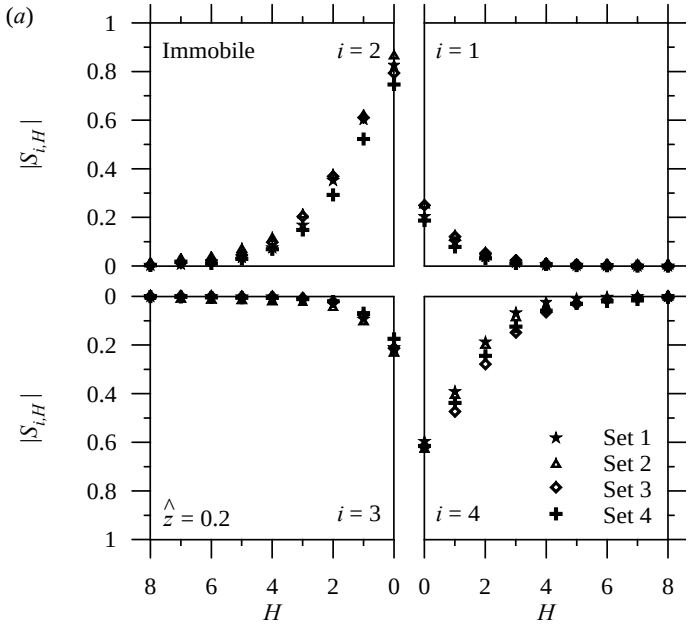

(A) Immobile bed

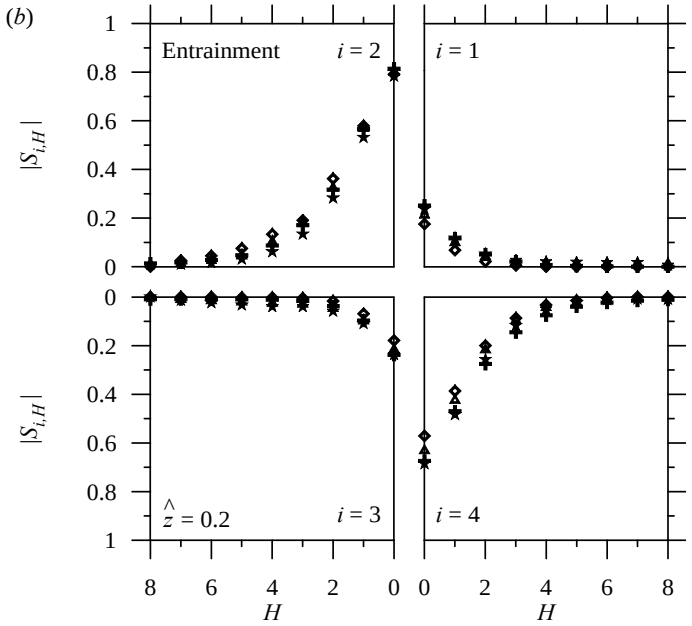

(B) Entrainment threshold bed

Variations of $|S_{i,H}|$ with H at $z/h = 0.2$

- The quadrant analysis of the data of velocity fluctuations corroborates that ejection and sweep events in the near-bed flow zone for immobile beds rescind each other giving rise to the outward interactions.

- Sweep events are the prevailing mechanism towards the sediment-entrainment.

- At the top of the wall-shear layer, ejection events are prevalent.

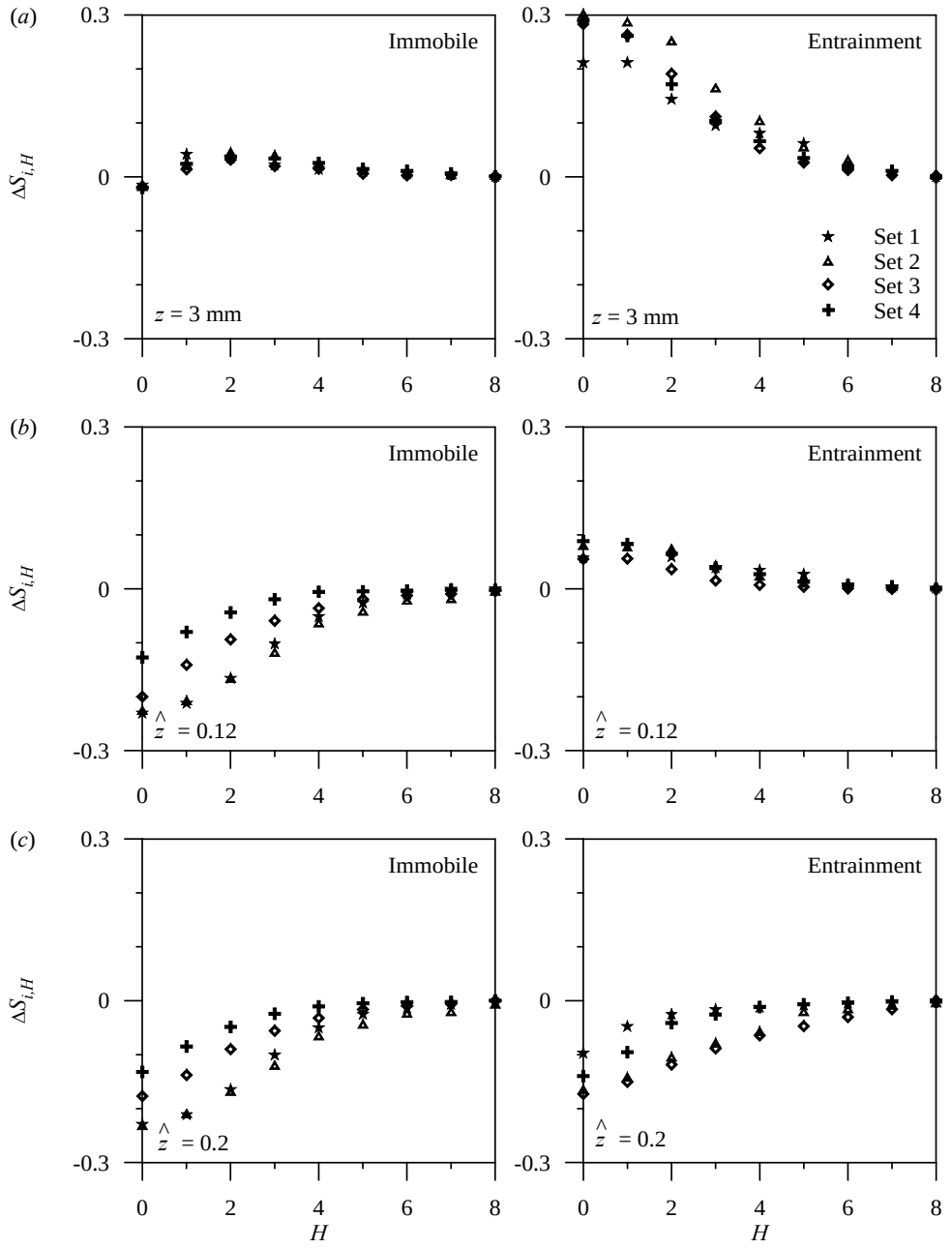

Variations of $\Delta Si,H$ *w*ith H

(A) at z = 3 mm

(B) at z/h = 0.12

(B) at z/h = 0. 2

Time-durations and frequencies of the ejection and sweep

The nondimensional mean time-durations of ejection and sweep events are represented by:

$$T_E = t_{Eu_*} / h \quad \text{and} \quad T_S = t_{Su_*} / h$$

T_E and T_S for immobile beds are greater than those for entrainment threshold beds.

The nondimensional mean frequencies of ejection and sweep events are

$$\hat{f}_E = i_E{}^{-1} h / u_* \quad \text{and} \quad \hat{f}_S = i_S{}^{-1} h / u_*$$

Frequency of ejection or sweep events for entrainment threshold beds is larger than that for immobile beds.

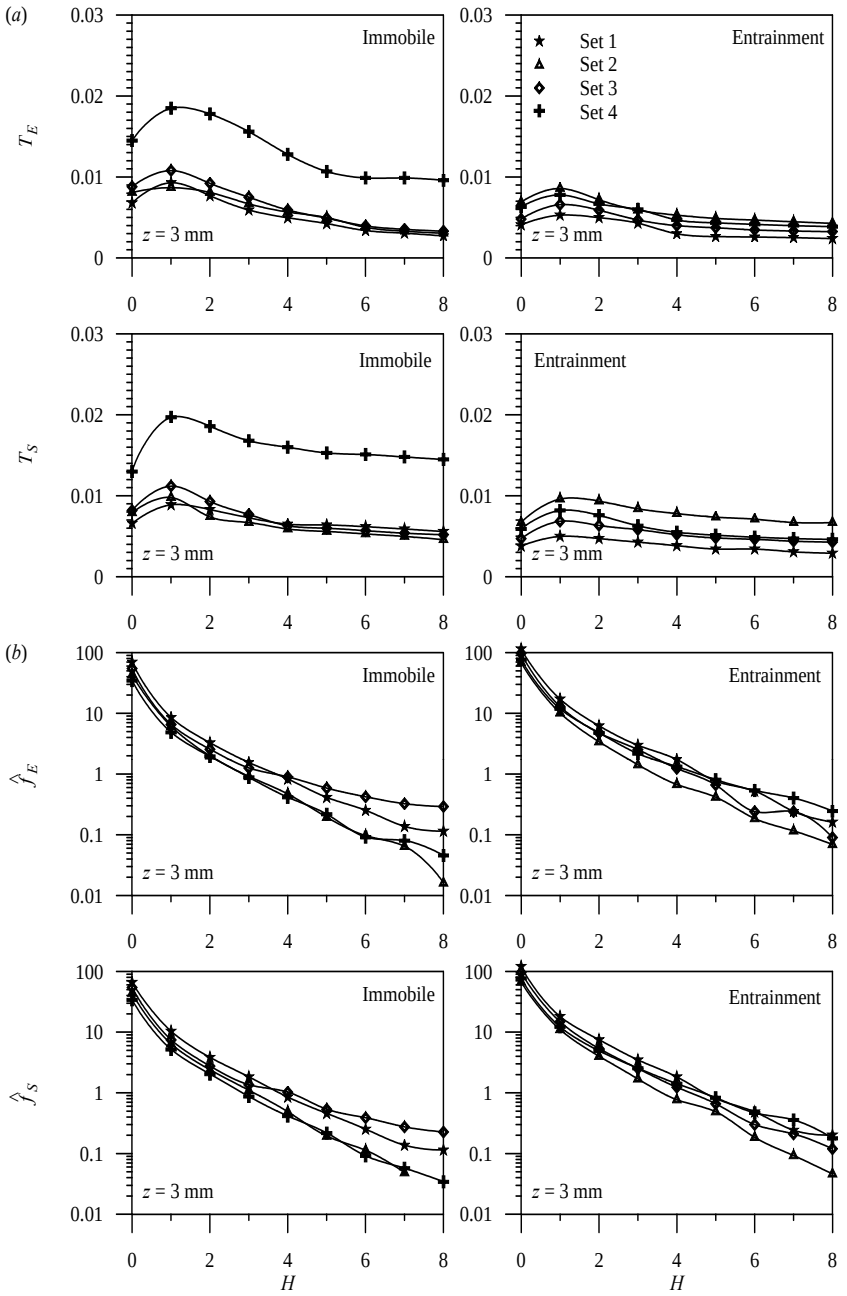

(A) Mean durations of $Q2$ and $Q4$ events

(B) Mean frequencies of $Q2$ and $Q4$ events

Mean duration and frequencies of $Q2$ and $Q4$ at z = 3 mm

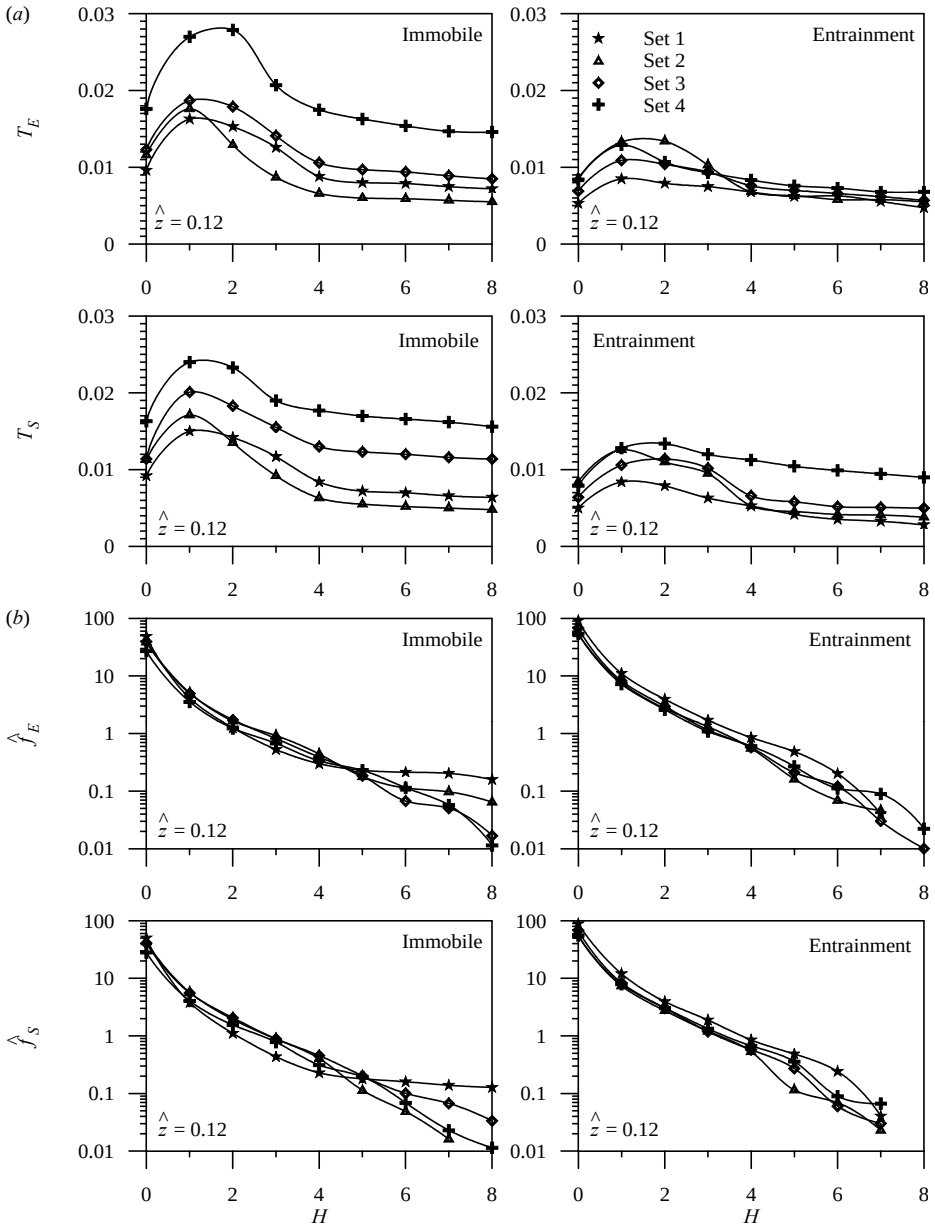

(A) Mean durations of $Q2$ and $Q4$ events

(B) Mean frequencies of $Q2$ and $Q4$ events

Mean duration and frequencies of $Q2$ and $Q4$ at z/h = 0.12

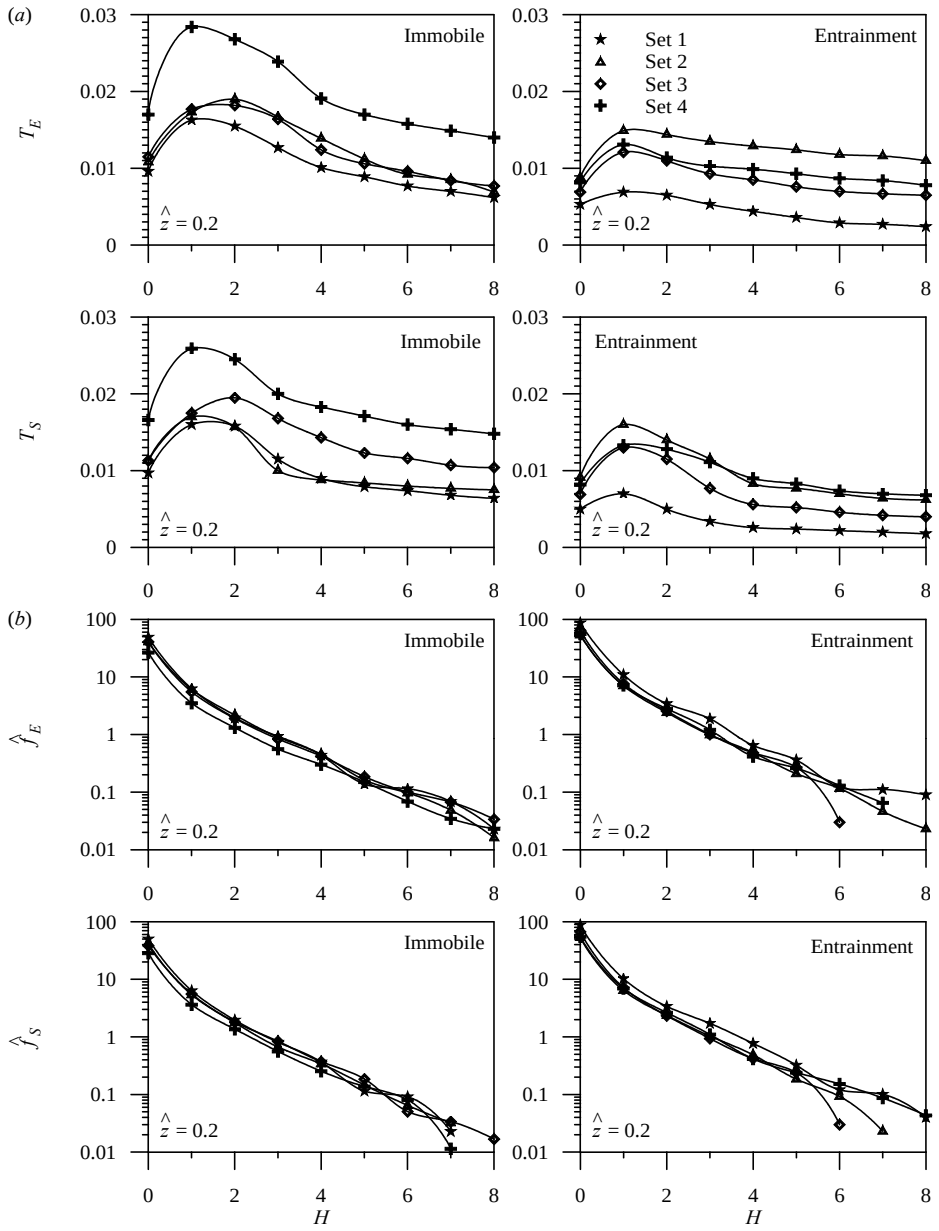

(A) Mean durations of $Q2$ and $Q4$ events

(B) Mean frequencies of $Q2$ and $Q4$ events

Mean duration and frequencies of $Q2$ and $Q4$ at z/h = 0.2

Conclusions

- Influence of an entrainment threshold of sediments on the turbulence characteristics is primarily confined to the wall-shear layer that characterises the near-bed flow zone. However, the turbulence characteristics in the outer-layer of flows are indistinguishable for immobile and entrainment threshold beds.

- In near-bed flow zone, there exists a departure in the distributions of the time-averaged streamwise velocity from the logarithmic law due to the roughness layer created by the sediment particles.

- The departure of the velocity data plots for immobile beds from the logarithmic law is higher than that for entrainment threshold beds.

- The near-bed distributions of the Reynolds shear stress for immobile and entrainment threshold beds also deviate from the linear law of the Reynolds shear stress having a relatively high damping in the distributions of the Reynolds shear stress for entrainment threshold beds.

- The streamwise turbulence intensities for immobile beds have smaller magnitudes than those for entrainment threshold beds within the wall-shear layer.

- The influence of sediment-entrainment on the vertical turbulence intensityis not apparent.

- The correlation coefficient for immobile beds exceeds that for entrainment threshold beds.

- Anisotropy analysis reveals that turbulence in flows over entrainment threshold beds possesses isotropy better than that over immobile beds, even though the turbulence in flows over both bed conditions is in general anisotropic (ratio of vertical to streamwise turbulence intensities $\approx 0.3 < 1$).

- In the spectral analysis, the velocity power spectra and the cross-power spectra are not influenced by the sediment-entrainment. The third-order correlations imply that a streamwise acceleration is prevalent during sediment- entrainment and is associated with a downward flux suggesting sweep events having a downward advection of the streamwise Reynoldsnormal stress.

- The increased near-bed positive value of streamwise flux of turbulent kinetic energy that migrates downstream and the negative value of vertical flux of turbulent kinetic energy that migrates downward is associated with the entrainment threshold of sediments.

- Energy budget identifies that for entrainment threshold beds, the turbulent dissipation is in excess of the turbulent production and the pressure energy diffusion becomes drastically negative.

- The quadrant analysis of the data of velocity fluctuations corroborates that ejection and sweep events in the near-bed flow zone of immobile beds rescind each other giving rise to the outward interactions; whereas sweep events are the prevailing mechanism towards the sediment-entrainment.

- At the top of the wall-shear layer, ejection events are prevalent.

- The mean-duration of sweep events for entrainment threshold beds is smaller (and more frequent) than that for immobile beds.

References

Best, J. 1992 *Sedimentology*, 39, 797-811.

Bey, A., Faruque, M. A. A. and Balachandar, R. 2007 *J. Hydraul. Eng.*, 133 (4), 414-430.

Buffington, J. M. and Montgomery, D. R. 1997 *Water Resour. Res.*, 33 (8), 1993-2030.

Cao, Z. 1997 *J. Hydraul. Eng.*, 123 (3), 233-236.

Choi, K. S. and Lumley, J. L. 2001 *J. Fluid Mech*., 436, 59-84.

Clifford, N. J., McClatchey, J. and French, J. R. 1991 *Sedimentology*, 38, 161-171.

Dey, S. 1999 *Appl. Math. Modelling*, 23 (5), 399-417.

Dey, S. 2003 *J. Hydraul. Res.*, 41 (4), 405-415.

Dey, S., Bose, S. K. and Sastry, G. L. N. 1995 *J. Hydraul. Eng*., 121 (12), 869-876.

Dey, S., Dey Sarker, H. K. and Debnath, K. 1999 *J. Eng. Mech.*, 125 (5), 545-553.

Dey, S. and Papanicolaou, A. 2008 *KSCE J. Civ. Eng.*, 12 (1), 45-60.

Dey, S. and Raikar, R. V. 2007 *J. Hydraul. Eng*., 133 (3), 288-304.

Drake, T. G., Shreve, R. L., Dietrich, W. E., Whiting, P. J. and Leopold, L. B. 1988 *J. Fluid Mech.*, 192, 193-217.

Egiazaroff, J. V. 1965 *J. Hydraul. Div.*, 91 (4), 225-247.

Fenton, J. D. and Abbott, J. E. 1977 *Proc. R. Soc. London*, *Ser. A*, 352, 523-537.

Gad-el-Hak, M. and Bandyopadhyay, P. R. 1994 *Appl. Mech. Rev.*, 47, 307-365.

Grass, A. J. 1970 *J. Hydraul. Div.*, 96 (3), 619-632.

Grass, A. J. 1971 *J. Fluid Mech.*, 50, 233-255.

Heathershaw, A. D. and Thorne, P. D. 1985 *Nature*, 316, 339-342.

Hinze, J. O. 1975 *Turbulence*. McGraw-Hill Book Company, New York.

Iwagaki, Y. 1956 *Trans. Jpn. Soc. Civ. Eng.*, 41, 1-21.

Irwin, H. P. A. H. 1973 *J. Fluid Mech*., 61, 33-63.

Kironoto, B. A. and Graf, W. H. 1994 *Proc. Inst. Civ. Eng.*, *Water*, *Maritime Energ.*, 106 (December), 333-344.

Kline, S. J., Reynolds, W. C., Schraub, F. A. and Runstadler, P. W. 1967 *J. Fluid Mech.*, 30, 741-773.

Kramer, H. 1935 *Trans. Am. Soc. Civ. Eng.*, 100, 798-838.

Krogstad, P. Å. and Antonia, R. A. 1999 *Exp. Fluids*, 27, 450-460.

Krogstad, P. A., Antonia, R. A. and Browne, L. W. B. 1992 *J. Fluid Mech.*, 245, 599-617.

Kurihara, M. 1948 *Rep. No.* 3, Vol. 4, Research Institute for Hydraulic Engineering, Kyushu University, Fukuota, Japan.

Lumley, J. L. and Newman, G. R. 1977 *J. Fluid Mech.*, 82, 161-178.

Lumley, J. L. 1978 *Adv. Appl. Mech.*, 18, 123-176.

Ling, C. H. 1995 *J. Hydraul. Eng*., 121 (6), 472-478.

Lu, H., Raupach, M. R. and Richards, K. S. 2005 *J. Geophys. Res.*, 110, D24114, doi: 10.1029/2005JD006418.

Lu, S. S. and Willmarth, W. W. 1973 *J. Fluid Mech.*, 60, 481-511.

Mantz, P. A. 1977 *J. Hydraul. Div.*, 103 (6), 601-615.

Neill, C. R. and Yalin, M. S. 1969 *J. Hydraul. Div.*, 95 (1), 585-588.

Nelson, J. M., Shreve, R. L., McLean, S. R. and Drake, T. G. 1995 *Wat. Resour. Res.*, 31 (8), 2071-2086.

Nakagawa, H. and Nezu, I. 1977 *J. Fluid Mech*., 80, 99-128.

Nezu, I. and Nakagawa, H. 1993 *Turbulence in Open-Channel Flows*. Balkema, Rotterdam, Netherlands.

Nikora, V. and Goring, D. 2000 *J. Hydraul*. *Eng.*, 126 (9), 679-690.

Nikora, V., Goring, D., McEwan, I. and Griffiths, G. 2001 *J. Hydraul*. *Eng.*, 127 (2), 123-133.

Papanicolaou, A. N. 2000 *Int. J. Fluid Dynamics*, 4, Article 2.

Papanicolaou, A. N., Diplas, P., Dancey, C. and Balakrishnan, M. 2001 *J. Eng. Mech.*, 127 (3), 211-218.

Robinson, S. K. 1991 *NASA TM-103859*.

Raupach, M. R. 1981 *J. Fluid Mech.*, 108, 363-382.

Raupach, M. R., Antonia, R. A. and Rajagopalan, S. 1991 *Appl. Mech. Rev.*, 44 (1), 1-25.

Schmeeckle, M. W., Nelson, J. M. and Shreve, R. L. 2007 *J. Geophys. Res.*, 112, F02003, doi: 10.1029/2006JF000536.

Schlichting, H. 1979 *Boundary Layer Theory*. McGraw-Hill Book Company, New York.

Shields, A. F. 1936 *Mitteilungen der Preussischen Versuchsanstalt für Wasserbau und Schiffbau,* 26, 5-24.

Song, T., Chiew, Y. M. and Chin, C. O. 1998 *J. Hydraul. Eng*., 124 (2), 165-175.

Song, T., Graf, W. H. and Lemmin, U. 1994 *J. Hydraul*. *Res.*, 32 (6), 861-876.

Streeter, V. L. and Wylie, E. B. 1983 *Fluid Mechanics*. McGraw-Hill Book Company, New York.

Sumer, B. M., Chua, L. H. C., Cheng, N. -S. and Fredsoe, J. 2003 *J. Hydraul. Eng.*, 129 (8), 585-596.

Sutherland, A. J. 1967 *J. Geophys. Res.*, 72, 6183-6194.

Thorne, P. D., Williams, J. J. and Heathershaw, A. D. 1989 *Sedimentology*, 36, 61-74.

van Rijn, L. C. (1984) *J. Hydraul. Eng.*, 110 (10), 1431-1456.

Voulgaris, G. and Trowbridge, J. H. 1998 *J. Atmos. Ocean. Technol.*, 15 (1), 272-289.

Yalin, M. S. and Karahan, E. 1979 *J. Hydraul. Div.*, 105 (11), 1433-1443.

Yeganeh-Bakhtiary, A., Gotoh, H. and Sakai, T. 2000 *J. Hydraul. Res.*, 38 (5), 389-398.

Yeganeh-Bakhtiary, A., Shabani, B., Gotoh, H. and Wang, S. S. Y. 2009 *J. Hydraul. Res.*, 47 (2), 203-212.

White, C. M. 1940 *Phil. Trans. Royal. Soc., Ser. A*, 174, 322-338.

Wiberg, P. L. and Smith, J. D. 1987 *Wat. Resour. Res.*, 23 (8), 1471-1480.

Zanke, U. C. E. 2003 *Int. J. Sediment Res.*, 18 (1), 17-31.

Thank You